Journal of Applied Science, Innovation & Technology (JASIT)

https://prakritimitrango.com

Research Article

Degradation of para-nitrophenol by green synthesised iron nanoparticles: Optimization of the process parameters and study of degradation kinetics

Shalu Rawat[1*] and Jiwan Singh[1]

[1]Department of Environmental Science, Babasaheb Bhimrao Ambedkar University, Lucknow-226025, India

ARTICLE INFOR: *Received: 15 May 2022; Revised: 10 June 2022; Accepted: 13 June 2022*
CORRESPONDING AUTHOR*: (S. Rawat) Email- shalurawat200@gmail.com*

Abstract

Dried waste leaves of *Plumeria* which is a garden waste was utilized for the preparation of leaf extract and it was used as a green reducing agent for the reduction of Ferric ions (present in $FeCl_3$ solution) into zerovalent iron nanoparticles. It is an easy, cost efficient and eco-friendly method of nanoparticle synthesis. The synthesised iron nanoparticles were characterized by the use of scanning electron microscope (SEM), energy dispersive X-ray spectroscopy (EDS), Fourier transform infrared spectroscopy (FTIR) and point of zero charge (pH_{ZPC}). The synthesised nanoparticles were agglomerated therefore the size appeared larger and they were mainly composed of iron and oxygen. FTIR analysis showed presence of several functional groups over the surface of nanoparticles that refers to its surface complexity. The pH_{ZPC} of the nanoparticles was found to be 5.2. The aqueous solution of para-nitrophenol (PNP) was treated in the Fenton-like degradation process using the synthesised iron nanoparticles as catalyst. PNP was efficiently removed from the aqueous solution with maximum percentage removal was 90.52 % with nanoparticle concentration 0.5 g/L, PNP concentration 10 mg/L, pH 3, H_2O_2 concentration 0.05 M and at 25 ˚C. The degradation of PNP was fitted best with pseudo-first-order kinetics.

Keywords: Iron nanoparticles; green synthesis; degradation; PNP; kinetics.

1. Introduction

Nanotechnology is one of the most promising and quickly expanding fields of science. Nanoparticles are specific due to their characteristic properties in comparison with their bulk materials such unique optical properties and high chemical reactivity (Paiva-Santos et al., 2021). Their characteristic properties are result of their extremely small size and huge surface to volume ratio (Jadoun et al., 2021). Nanoparticles have wide area of application, they are used in magnetic and microelectronic devices, photocatalyst, electrocatalysts, biomedical field and powder metallurgy (Salem and Fouda, 2021). Techniques like chemical reduction, laser ablation, pyrolysis, lithography and electrochemical synthesis have been used for the synthesis of nanoparticles. However, these techniques pose high synthesis cost as well as they have dangerous effects on environment because of usage of toxic chemicals and harsh reaction conditions (Rafique et al., 2017). Utilization of plant based materials and microorganisms for the synthesis of nanoparticles is a sustainable, environmentally safer and pocket friendly. Nanoparticle synthesis by microorganisms demands more time, cautious handling and high maintenance, whereas, nanoparticles synthesis by plants is a fast and easy reaction moreover, phytochemicals of plants not only reduce the metal ions into nanoparticles but also cap them with organic compounds which provide them stability (Hosny et al., 2021; Karthik et al., 2022).

The green synthesis of different metallic nanoparticles including silver nanoparticles, copper nanoparticles, iron nanoparticles and zinc oxide nanoparticles has been reported by the use of several plants extracts like leaves of *Azadirachta indica* (Nagar and Devra, 2018), *Enicostemma axillare* (Raj et al., 2018), Laurus nobilis L. (Fakhari et al., 2018), *Moringa oleifera* (Katata-Seru et al., 2018), *Thymus kotschyanus* (Hamelian et al., 2018), *Diospyros lotus* (Hamedi and Shojaosadati, 2019), seeds of *Tectona grandis* (Rautela et al., 2019), turmeric extracts (Alsammarraie et al., 2018), leaf and root of *Berberis vulgaris* (Behravan et al., 2019), flower of *Avicennia marina* (Karpagavinayagam and Vedhi, 2019), and red peanut skin extract (Pan et al., 2020). In the present research work, we have synthesised iron nanoparticles by the aqueous extract of dried *Plumeria* leaves. Those green synthesised iron nanoparticles were applied for the removal of para-nitrophenol from water by heterogeneous Fenton-like reaction, the removal process was optimized and analysed by the application of degradation kinetics.

2.0 Materials and methods

2.1 Materials

The analytical grade chemicals were utilised in this work like anhydrous ferric chloride ($FeCl_3$), para-nitrophenol ($C_6H_5NO_3$), hydrogen peroxide (H_2O_2), sodium hydroxide (NaOH), hydrochloric acid (HCl), and other chemicals and reagents were provided by Thermo Fisher Scientific. The dried leaves of *Plumeria* were collected from the Babasaheb Bhimrao Ambedkar University campus, Lucknow, India.

2.2 Synthesis and characterizations of nanoparticles

A detailed synthesis method of iron nanoparticles using extract of dead *Plumeria* leaf is given in our previous work Rawat and Singh (2021). In brief the preparation of leaf extract was done by heating a mixture of dried leaf powder and deionized water at 80˚C for 1 h (DW) (leaf powder(g): DW(mL)= 3:50) which was then vacuum filtered and filtrate was used for reducing and capping of iron nanoparticles. The leaf extract was mixed in the 0.1 M aqueous solution of $FeCl_3$

in the ratio of 3:1 with constant stirring and then pH of the mixture was adjusted to 6. Reaction mixture turns intense black which represents the synthesis of zerovalent iron nanoparticle. The nanoparticles were then separated from the colloidal suspension by centrifugation, washed with distilled water and ethanol, dried, crushed into fine powder and stored for characterization and application. The nanoparticles were named *Plumeria* synthesised iron nanoparticles (Pl-INPs). The characterization of Pl-INPs was done by SEM (model number JSM 4490, JEOL, Japan), along with EDS and FTIR (NICOLET 6700, Thermo Fischer Scientific, USA). The pH_{ZPC} of the Pl-INPs was determined by the method described by Mishra et al. (2019).

2.3 Degradation of PNP

Degradation experiments were performed in 250 mL Erlenmeyer flask. For degradation a definite concentration of Pl-INPs was added in the 50 mL aqueous solution of PNP (10 mg/L), pH of the solution was 3, H_2O_2 concentration was 0.02 M, and then the reaction mixture was shaked at 80 RPM in an orbital shaker for definite contact time at room temperature. A 5 mL aliquot was take out after different time periods, centrifuged and analysed for residual PNP concentration in the solution by UV-Visible spectrophotometer (at 317 nm). The degradation percentage was determined by following reaction:

$$\boldsymbol{Degradation}\ \% = \frac{\boldsymbol{C_0 - C_t}}{\boldsymbol{C_0}} \times \mathbf{100} \qquad (\mathbf{1})$$

Where, C_0 and C_t are initial and residual concentration of PNP after degradation reaction, respectively. The optimization of Pl-INPs concentration, pH, H_2O_2 concentration, initial PNP concentration, reaction time and temperature for PNP degradation was done in this study.

2.4 Degradation kinetics

The degradation study data of PNP was analysed by the application of pseudo-first-order and pseudo-second-order kinetics. The linear equation for the pseudo-first-order and pseudo-second-order kinetic is represented in equation (2) and (3) (Rawat et al., 2021).

$$\boldsymbol{ln\left({C_t}/{C_0}\right) = -k_1 t} \qquad (\mathbf{2})$$

$$\boldsymbol{{1}/{C_t} = \left(\frac{1}{C_0}\right) + k_2 t} \qquad (\mathbf{3})$$

Where, C_0 is initial and C_t is residual concentration of PNP after degradation, respectively. k_1 and k_2 depicts pseudo-first-order and pseudo-second-order rate constant, respectively.

2.5 Regeneration of Pl-INPs

The regeneration of the Pl-INPs was done for five cycles. After application in first cycle the nanoparticles were separated from the reaction solution and washed with distilled water followed by drying in an oven overnight after that PI-INPs were applied in the second degradation cycle. Similarly the nanoparticles were recycled five times.

3.0 Results and discussion

3.1 Characterization of the nanoparticles

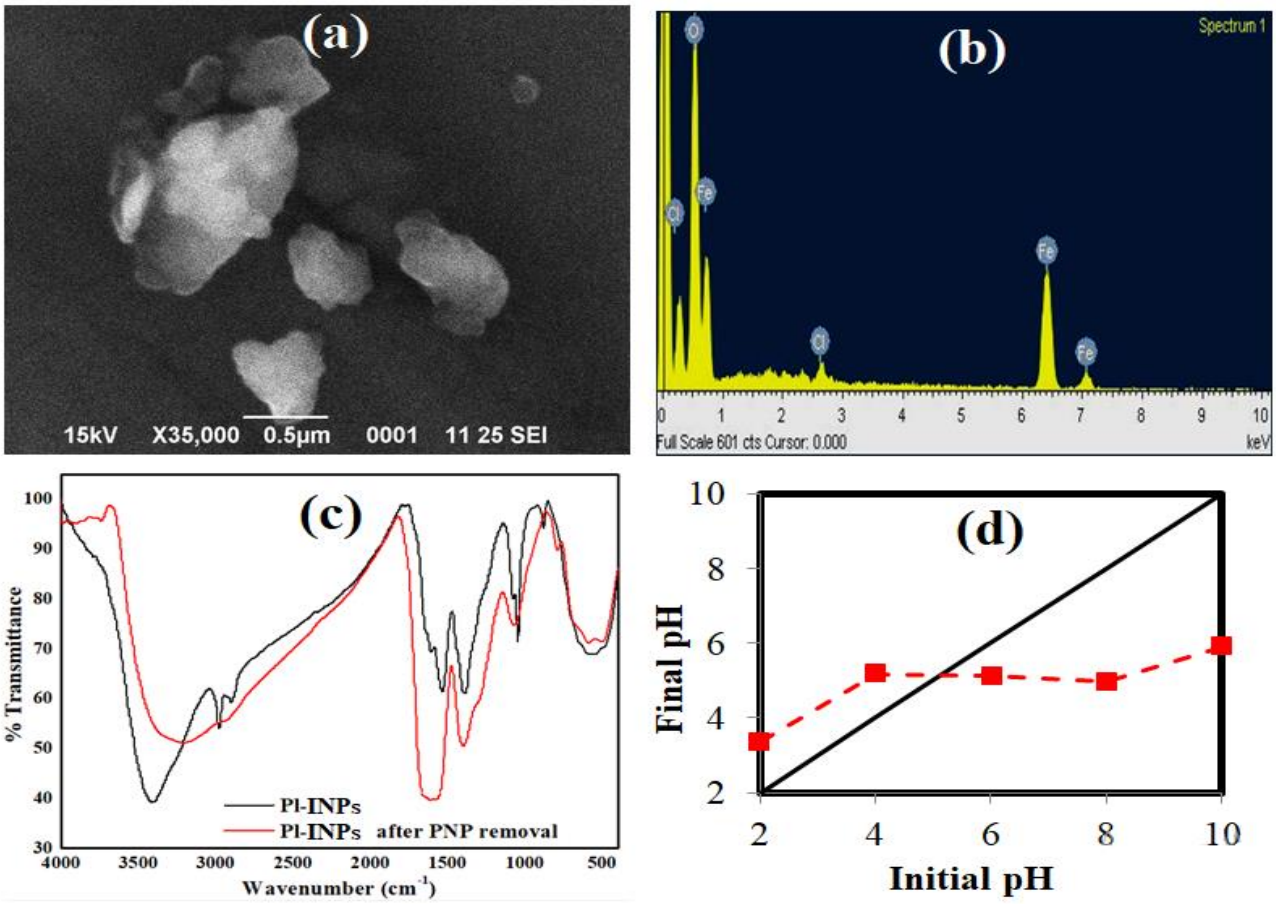

Fig. 1 a) SEM analysis, b) EDS, c) FTIR and d) pH_{ZPC} analysis of Pl-INPs

The SEM analysis shows clumping of nanoparticles due to which their particle size has increased (Fig. 1a). The EDS analysis represents the presence of Fe and O in the nanoparticle, the oxygen is present due to the oxidation of iron by reaction with ambient environment; however, a small amount of Cl present in EDS analysis may appear due to some impurities (Fig. 1b). FTIR analysis before and after removal PNP is represented in Fig. 1c. Several peaks appeared in the graph corresponding to different functional groups like peak appeared ~3422 cm^{-1} correspond to the –OH stretching, 1718.27 cm^{-1} correspond to –CO group, other group that were present are C=C bond, –C-N bond and –CH bond. A broad peak in between 600-400 cm-1 is representative of Fe-O bond in the Pl-INPs (Kouhbanani et al., 2018). The result of pH_{ZPC} is shown in Fig. 1d pH_{ZPC} was found to be 5.2.

3.2 Optimization of phenol and PNP degradation

The concentration of Pl-INPs was optimize in the range of 0.05 to 1 g/L (Fig. 2a) at pH 3, temperature 25 ˚C and contact time 4 h. A maximum degradation of PNP was found to be 85.2 ± 1.5 % at 0.75 g/L which was used for further degradation experiments of PNP. The study revealed a decrease in removal percentage on increasing the Pl-INPs concentration continuously that occur because of agglomerating tendency of nanoparticle in the reaction mixture when present in higher concentration that reduces the active sites for OH˚ generation (Kuang et al., 2013). Optimization of H_2O_2 concentration was done in the range of 0.001 to 0.1 M result shows that the degradation was increased with an increasing concentration of H_2O_2 (Fig. 2b) due to increase in the generation of OH˚ radicals (Al-Musawi et al., 2019). On increasing further concentration of H_2O_2 above the optimum level the number of generated OH˚ radicals will overcome the pollutant molecules to be degraded hence the degradation percentage became almost constant after 0.05 M H_2O_2 concentration. Degradation was tested in the pH range 2 to 7 results are shown in Fig. 2c which represents a wide range of pH (3-6) for the application Pl-INPs for Fenton like degradation. However, the degradation percentage was decreased slightly at higher pH. The concentration of PNP was studied from 10 mg/L to 50 mg/L. As shown in Fig. 2d, the degradation was almost unaffected with the increase in the initial concentrations up to 30 mg/L. After increase in concentration of PNP more than 30 mg/L the removal percentage was decreased, and minimum degradation was achieved at 50 mg/L. Increasing PNP amount and keeping constant amount of nanoparticles and H_2O_2, the amount of generated OH˚ radicals was also constant, while the pollutant molecules to be degraded keep increasing this led to the decrease in degradation due to insufficient supply of OH˚ radicals (Guo et al., 2020).

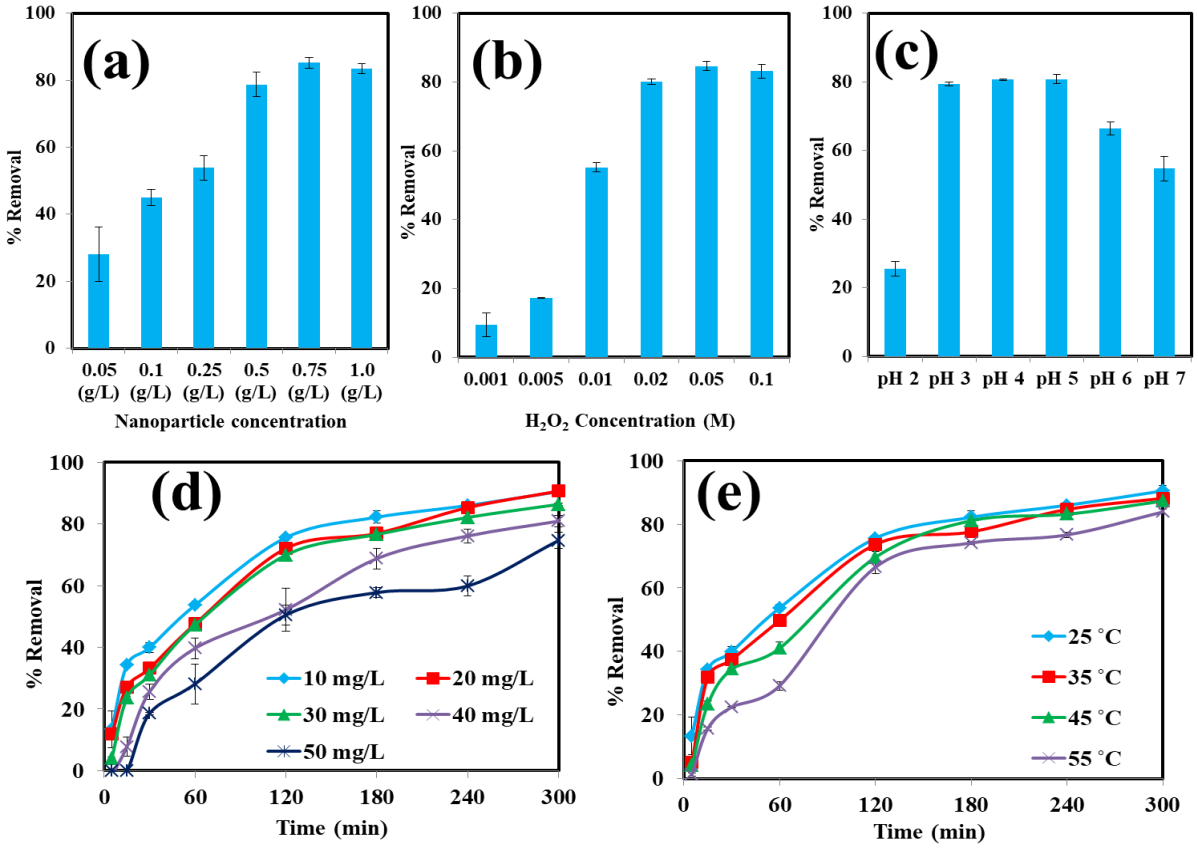

Fig. 2 a) Optimization of Nanoparticle concentration, b) optimization of H_2O_2 concentration, c) optimization of pH, d) optimization of PNP concentration and e) optimization of temperature.

The degradation was carried out for 300 min with regular time intervals this study was done along with the optimization of initial pollutant concentration. The results show that the degradation was increasing with an increasing reaction time. Degradation was fast in initial 120 min after that it was comparatively slower, similar observations were also reported by Dolatabadi et al. (2019). In starting, a large number of OH˚ radicals were generated due to higher concentration of H_2O_2 and vacant active sites on the Pl-INPs. While after some time some amount of H_2O_2 get consumed and some active sites on the Pl-INPs get masked with the by-products formed in the reaction so the production of OH˚ radical get slow down with time which eventually reduced the speed of the degradation reaction. The results of temperature

study shows a slight decrease in the degradation (Fig. 2e) at higher temperature, the reaction of OH˚ radical generation may get hampered due to which the degradation decreased slightly.

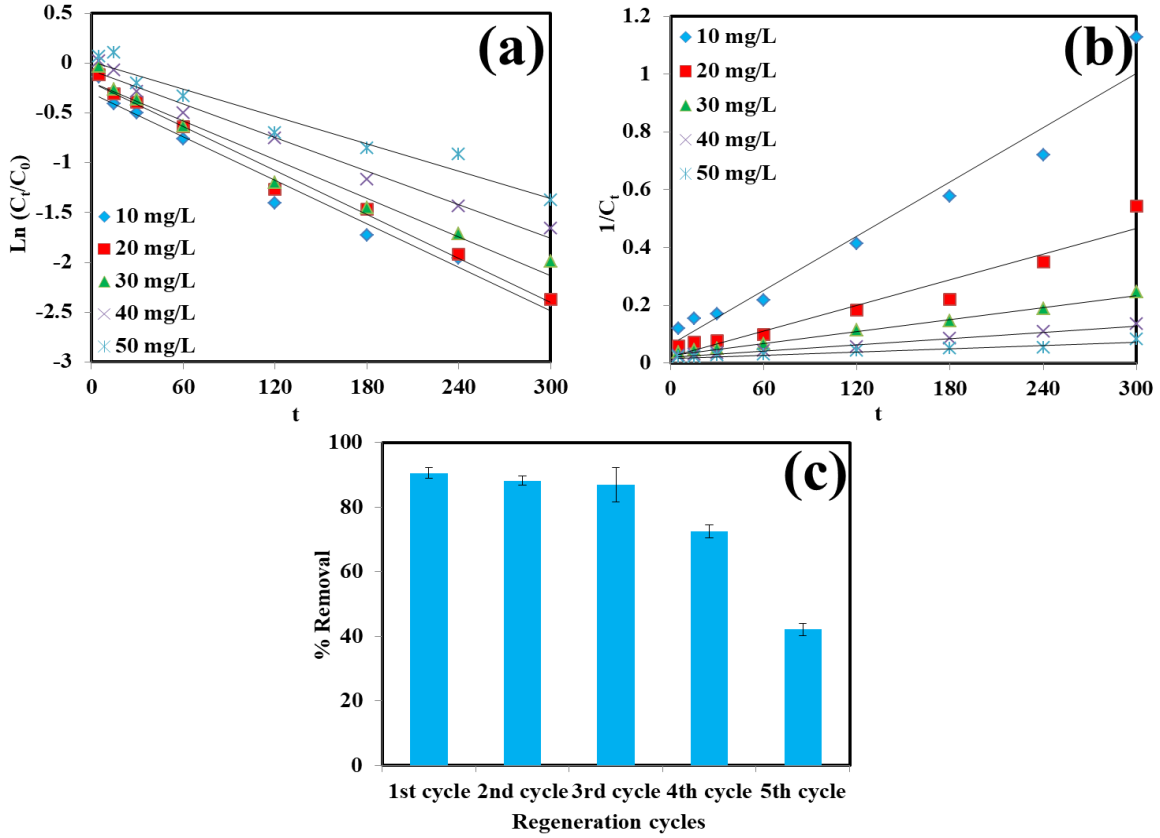

Fig. 3 a) Pseudo-first-order kinetic plots, b) pseudo-second-order kinetic plots for PNP degradation and c) Regeneration of Pl-INPs

3.3 Degradation kinetics

The values of reaction rate constants for both the kinetics and their respective R^2 values are provided in the Table 1. Fig. 3a and 3b show the plots for pseudo-first and second-order kinetics, respectively. By evaluation of the R^2 values it was observed that the degradation data fitted best with the pseudo-first-order kinetics.

Table 1 Values of degradation kinetics parameters

	Pseudo-first order kinetics		Pseudo-second-order kinetics	
C_0 (mg/L)	k_1	R^2	k_2	R^2
10	0.0076	0.976	0.0195	0.922
20	0.0073	0.753	0.0053	0.604
30	0.006	0.766	0.0022	0.594
40	0.0041	0.710	0.0007	0.672
50	0.0015	0.766	0.002	0.754

3.4 Regeneration and recycling of the Pl-INPs

Fig. 3c depicts the regeneration of the Pl-INPs, it can be observed from the figure that the degradation continuously kept on decreasing with increasing the number of regeneration cycles. In the process of recycling, some amount of catalyst also get lost in run off that reduces the degradation efficiency. Also iron get corroded in aqueous solution by the production of hydroxide layer which easily leached out and exposes the inner layer of iron for hydroxide formation resulting in eventual loss of iron that reduces the degradation efficiency of iron nanoparticles over time (Bokare et al., 2008).

4.0 Conclusion

In this study, the green synthesised iron nanoparticles were found to be an effective heterogeneous Fenton catalyst. Approximately 90% PNP was observed to be removed in this process and the removal was less effected by the increased in initial PNP concentration upto 30 mg/L. Moreover, the removal of PNP was slightly decreased with an increase in operating temperature up to 55 ˚C. It was observed that the degradation efficiency of PNP was observed good at pH range 3-5 unlike the conventional Fenton process which are feasible only at pH 3, this property make the application of nanoparticles in wastewater treatment with a wider range of pH. The kinetic study suggested the degradation was pseudo-first-order kinetic driven reaction. The nanoparticles were recyclable and had good catalytic properties for initial three cycles.

Author contribution: Shalu Rawat (Ph.D. student) has conducted all experiments, and drafted the manuscript and **Dr. Jiwan Singh** (Asst. Professor) has supervised the work, revised and edited the manuscript.

Acknowledgment: This study was financially supported by Science and Engineering Research Board (SERB), Department of Science and Technology (DST), Government of India (Reference no. ECR/2016/001924), University Grant Commission (UGC), Government of India (UGC-BSR Research startup grant project No. F. 30–382/2017, BSR), and Junior Research Fellowship (UGC-Ref. No: 3840/(NET-

DEC 2018) from University Grant Commission (UGC), New Delhi.

Conflict of interest: Authors declare no conflict of interest.

References

Abubaker, J., Risberg, K., Jönsson, E., Dahlin, A.S., Cederlund, H., Pell, M., 2015. Shortterm effects of biogas digestates and pig slurry application on soil microbial activity. Appl. Environ. Soil Sci. 2015, 1–15.

Al-Musawi, T.J., Kamani, H., Bazrafshan, E. et al., 2019. Optimization the Effects of Physicochemical Parameters on the Degradation of Cephalexin in Sono-Fenton Reactor by Using Box-Behnken Response Surface Methodology. Catal. Lett. 149, 1186–1196.

Alsammarraie, FK., Wang, Wei., Zhou, P., Mustapha, A., Lin, M., 2018. Green synthesis of silver nanoparticles using turmeric extracts and investigation of their antibacterial activities. Colloid Surf. B. 171, 398–405.

Behravan, M., Panahi, A.H., Naghizadeh, A., Ziaee, M., Mahdavi, R., Mirzapour, A., 2019. Facile green synthesis of silver nanoparticles using Berberis vulgaris leaf and root aqueous extract and its antibacterial activity. Int. J. Biol. Macromol. 124, 148-154.

Bokare, A.D., Chikate, R.C., Rode, C.V., Paknikar, K.M., 2008. Iron-nickel bimetallic nanoparticles for reductive degradation of azo dye Orange G in aqueous solution. Appl. Catal. B. 79(3), 270–278. doi:10.1016/j.apcatb.2007.10.033

Dolatabadi, M., Ahmadzadeh, S., Ghaneian, M.T., 2019. Mineralization of mefenamic acid from hospital wastewater using electro-Fenton degradation: Optimization and identification of removal mechanism issues. Environ. Prog. Sustain. Energy. doi:10.1002/ep.13380

Fakhari, S., Jamzad, M., Kabiri F.H., 2019. Green synthesis of zinc oxide nanoparticles: a comparison. Green Chem. Lett. Rev. 12(1), 19-24.

Guo, B., Xu, T., Zhang, L., Li, S., 2020. A heterogeneous fenton-like system with green iron nanoparticles for the removal of bisphenol A: Performance, kinetics and transformation mechanism. J. Environ. Manage. 272, 111047.

Hamedi, S. Seyed A.S., 2019. Rapid and Green Synthesis of Silver Nanoparticles Using Diospyros lotus Extract: Evaluation of their Biological and Catalytic Activities. Polyhedron,. S0277538719304802. doi:10.1016/j.poly.2019.07.010

Hamelian, M., Zangeneh, M.M., Amisama, A., Varmira, K., Veisi, H., 2018. Green synthesis of silver nanoparticles using Thymus kotschyanus extract and evaluation of their antioxidant, antibacterial and cytotoxic effects. Appl. Organomet. Chem. 32 (9), e4458. doi:10.1002/aoc.4458

Hosny, M., Fawzy, M., Abdelfatah, A.M., Fawzy, E.E., Eltaweil, A.S., 2021. Comparative study on the potentialities of two halophytic species in the green synthesis of gold nanoparticles and their anticancer, antioxidant and catalytic efficiencies. Adv. Powder Technol. 32(9), 3220–3233. doi:10.1016/j.apt.2021.07.008

Jadoun, S., Arif, R., Jangid, N.K., Meena, R.K., 2021. Green synthesis of nanoparticles using plant extracts: A review. Environ. Chem. Lett. 19(1), 355-374.

Karpagavinayagam, P., Vedhi, C., 2019. Green synthesis of iron oxide nanoparticles using Avicennia marina flower extract. Vacuum, 160, 286-292.

Karthik, K.V., Raghu, A.V., Reddy, K.R., Ravishankar, R., Sangeeta, M., Shetti, N.P., Reddy, C.V., 2022. Green synthesis of Cu-doped ZnO nanoparticles and its application for the photocatalytic degradation of hazardous organic pollutants. Chemosphere, 287, 132081. doi:10.1016/j.chemosphere.2021.132081

Katata-Seru, L., Moremedi, T., Aremu, O.S., Bahadur, I., 2018. Green synthesis of iron nanoparticles using Moringa oleifera extracts and their applications: removal of nitrate from the water and antibacterial activity against Escherichia coli. J. Mol. Liq. 256, 296-304.

Kouhbanani, M.A.J., Beheshtkhoo, N., Amani, A.M., Taghizadeh, S., Beigi, V., Bazmandeh, A.Z., Khalaf, N., 2018. Green synthesis of iron oxide nanoparticles using Artemisia vulgaris leaf extract and their application as a heterogeneous Fenton-like catalyst for the degradation of methyl orange. Mater. Res. Express. 5(11), 115013.

Kuang, Y., Wang, Q., Chen, Z., Megharaj, M., Naidu, R., 2013. Heterogeneous Fenton-like oxidation of monochlorobenzene using green synthesis of iron nanoparticles. J. Colloid Interface Sci. 410, 67-73.

Mishra, S., Yadav, S.S., Rawat, S., Singh, J., Koduru, J.R., 2019. Corn husk derived magnetized activated carbon for the removal of phenol and para-nitrophenol from aqueous solution: Interaction mechanism, insights on adsorbent characteristics, and isothermal, kinetic and thermodynamic properties. J. Environ. Manage. 246, 362-373.

Nagar, N., Devra, V., 2018. Green synthesis and characterization of copper nanoparticles using Azadirachta indica leaves. Mater. Chem. Phys. S0254058418302694–. doi:10.1016/j.matchemphys.2018.04.007

Paiva-Santos, A.C., Herdade, A.M., Guerra, C., Peixoto, D., Pereira-Silva, M., Zeinali, M., Veiga, F., 2021. Plant-mediated green synthesis of metal-based nanoparticles for dermo-pharmaceutical and cosmetic applications. Int. J. Pharm. 597, 120311.

Pan, Z., Lin, Y., Sarkar, B., Owens, G., Chen, Z., 2020. Green synthesis of iron nanoparticles using red peanut skin extract: Synthesis mechanism, characterization and effect of conditions on chromium removal. J. Colloid Interface Sci. 558, 106-114.

Rafique, M., Sadaf, I., Rafique, M. S., Tahir, M. B., 2017. A review on green synthesis of silver nanoparticles and their applications. Artif. Cells Nanomed. Biotechnol. 45(7), 1272-1291.

Raj, S., Mali, S. C., Trivedi, R., 2018. Green synthesis and characterization of silver nanoparticles using Enicostemma axillare (Lam.) leaf extract. Biochem. Biophys. Res. Commun. 503(4), 2814-2819.

Rautela, A., Rani, J. Debnath (Das), M., 2019. Green synthesis of silver nanoparticles from *Tectona grandis* seeds extract: characterization and mechanism of antimicrobial action on different microorganisms. J. Anal. Sci. Technol. 10 (5), 1-10. https://doi.org/10.1186/s40543-018-0163-z

Rawat, S., Singh, J., 2021. Green Synthesis of Iron Nanoparticles Using Plumeria and Jatropha: Characterization and Investigation of Their Adsorption, Regeneration and Catalytic Degradation Efficiencies. BioNanoSci. 11, 1142–1153.

Rawat, S., Singh, J., Koduru, J.R., 2021. Effect of ultrasonic waves on degradation of phenol and para-nitrophenol by iron nanoparticles synthesized from Jatropha leaf extract. Environ. Technol. Inno. 24, 101857.

Salem, S.S., Fouda, A., 2021. Green Synthesis of Metallic Nanoparticles and Their Prospective Biotechnological Applications: an Overview. Biol. Trace. Elem. Res. 199, 344–370.

Cite this article:

Rawat, S., Singh, J., 2022. Degradation of para-nitrophenol by green synthesised iron nanoparticles: Optimization of the process parameters and study of degradation kinetics. J. Appl. Sci. Innov. Technol. 1 (1), 21-26.